Supporting Information

Designing Caps for Colloidal Au Nanoparticles

Xiaoli Tian, Jianpeng Zong, Yusai Zhou, Dapeng Chen, Jia Jia, Shuaibin Li, Xiaochen Dong, Yuhua Feng* and Hongyu Chen*

Chemicals. All chemical reagents were used as received unless otherwise noted. Hydrogen tetrachloroaurate (III) trihydrate ($HAuCl_4$, 99.9%, Au 49% on metals basis, Alfa Aesar); 4.5-diphenyl-2-imidazolethiol (DPI, 0.97%) was purchased from Sigma-Aldrich; Myristyltrimethylammonium bromide (MTAB, > 0.98%), 2,7-dihydroxynaphthalene (DHN, 99.0%) were all purchased from Tokyo Chemical Industry Co., Ltd (TCI); N,N-dimethylformamide (DMF), Sodium hydroxide (NaOH) and ethanol (EA) were all purchased from Sinopharm Chemical Reagent Co. Ltd; Sodium citrate tribasic dihydrate (99.0%) were purchased from Alfa Aesar; Deionized water (resistance > 18.2 $M\Omega \bullet cm^{-1}$) was used in all reactions. Copper specimen grids (300 mesh) with formvar/carbon support film were purchased from Beijing Zhongjingkeyi Technology Co., Ltd.

Characterizations. SEM images were collected on Quanta 250 FEG Scanning Transmission Electron Microscopy operated under 30 kV. TEM images were collected from Talos L120C transmission electron microscope operated at 120 kV. Absorption spectra were collected on a Cary 100 UV-Vis-NIR spectrophotometer. Raman spectra and SERS were collected by using the as-synthesized sample solutions in a quartz cuvette (path length = 1.00 cm) on a portable Raman analyzer (Accuman SR-510 Pro) equipped with 785 nm laser (350 mW). The integration times are 3s or 10s for different samples. HRTEM were collected on a JEOL JEM-3000F transmission electron microscope. High-angle annular dark-field scanning transmission electron microscopy (HAADF-STEM) image and EDS were collected from the JEOL JEM-2100 transmission electron microscopy.

Synthesis and surface modification of gold nanoparticles. Au seed NPs in 60 nm diameter were synthesized via a seeded growth method derived from the citrate-reduction method.[1] As direct ligand exchange between citrate and hydrophobic thiol ligand causes serious aggregation, we first replace the citrate with myristyltrimethylammonium bromide (MTAB). The pre-synthesized 200 mL sodium citrate stabilized 60 nm AuNPs solution was divided into 5 mL centrifuge tubes and centrifuged at 3500 rpm/min for 10 minutes. Disperse all precipitates in 100 mL of deionized water. 100 mL (20 mM) MTAB aqueous solution was placed on a magnetic stirrer for stirring at 1400 rpm/min. After the MTAB is completely dissolved, 100 mL the AuNPs dispersion is added dropwise to the MTAB solution under stir, stirring is continued for 1 hour after the dropwise addition is completed. The resulting mixture is highly stable and used as the stock solution for all of the subsequent syntheses.

Synthesis and characterization of Au Nanoparticles with different caps. To 1 mL solution of MTAB-stabilized 60 nm Au nanoparticles, a strong hydrophobic ligand 4,5-diphenyl-2-imidazolethiol (DPI) was used in combination with a cationic surfactant MTAB under vigorous vortexing. The solution was

incubated at 60 ºC for 2 h. After cooling to room temperature, NaOH, 2,7-dihydroxynaphthalene (DHN) and $HAuCl_4$ were added quickly to the above solution under vigorous stirring. For clarification, the synthetic conditions for different structures were listed in table 1. The mixed solution was allowed to stand at room temperature for at least 12 hours, so that $HAuCl_4$ was fully reduced. and finally Au nanoparticles with different cap structures were obtained. The products were isolated by centrifugation and characterized by transmission electron microscopy (TEM) and scanning electron microscopy (SEM). Two-time diluted sample solutions without purification were used for UV-Vis-NIR absorption spectral collection.

Table S1. Synthetic conditions for Au caps structures

Caps	HAuCl4	NaOH	DHN	DPI
mortarboard	0.6	0.83	1.2	0.2
beret hats	0.6	2.64	1.2	0.2
helmets	0.6	3.96	1.2	0.2
crowns	0.6	3.96	4.6	0.2
antler hats	0.6	3.96	9.23	0.2
antenna	0.6	3.96	13.8	0.2

Note: all the regent concentrations (mmol/L) are their final concentration in growth solution.

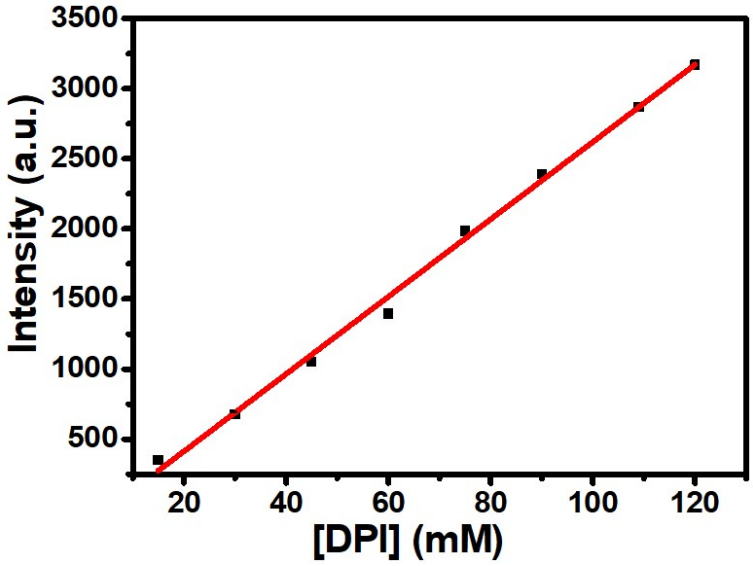

Figure S1. Linear fit for Raman intensity of DPI ligand in DMF.

The calculation of SERS enhancement factor. We employed the strongest peak 1604 cm^{-1} of DPI to calculate the SERS enhancement factor of mortarboard. The calculation is based on the following Equation 1:

$$EF = (I_{SERS} \times C_{bulk})/ (I_{bulk} \times C_{SERS}) \quad (1)$$

Where I_{SERS} and I_{bulk} are the Raman intensities of the 1604 cm^{-1} peak for mortarboard and pure DPI solution, C_{SERS} and C_{bulk} are the concentrations of DPI on/in mortarboard and in pure solution. For the selection of I_{bulk}, we made a 0.12 M DPI solution. By stepwise diluting, we got titration plots of SERS intensities vs DPI (Figure S1). Within this titration plots, the I_{bulk} should be in the range with fine linear ship between Raman intensity and DPI. Thus, we selected Raman intensity corresponding to 0.109 M as I_{bulk}.

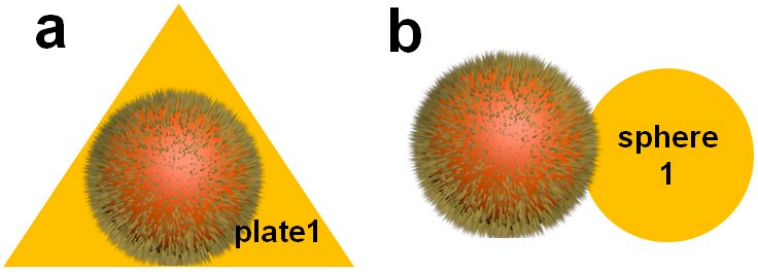

Figure S2. Two types of calculation area: a) triangular naoplate. b) sphere.

According to the literature,[1] the concentration of the as-prepared Au NPs is C_0 = 142.7 pM. So the NP concentration of the mortarboard nanostructure, C = 0.806 C_0 = 115 pM. Surface area of mortarboard structure in the solution is composed of two types of calculation area: triangular naoplate and sphere.

$S_{plate} = S_{plate1} + S_{seed} = 1 / 2 \times a \times h_1 \times 2 + 4 \times \pi \times r^2 = 1 / 2 \times 10^2 \times 127 \times 2 + 4 \times \pi \times 30^2 = 24258\ nm^2$.

$S_{sphere} = S_{seed} + S_{sphere1} - S_{interface} = 2 \times 4 \times \pi \times r^2 - 2 \times \pi \times r \times h^2 \times 2 = 18840\ nm^2$. $S_{interface}$ is the area at the interface of the sphere and Au seed.

According to the literature,[2] surface area of one ligand binding site on Au surface: S = 0.2155 nm^2.

Total number of ligand binding sites on the surface of NP = $C \times 0.64 \times S_{plate}/0.2155 + C \times 0.36 \times S_{sphere}/0.2155 = 9.7 \times 10^3$ nM.

$I_{SERS} = 2.08 \times 10^5$ counts, I_{bulk} = 2877 counts, C_{bulk} = 109 mM

$EF = (I_{SERS} \times C_{bulk})/(I_{bulk} \times C_{SERS}) = 8.1 \times 10^5$.

Calculation of photothermal conversion efficiency. The photothermal conversion efficiency of antler hat and antennas were calculated by following method:[3]

$$\eta = \frac{hS(T_{Max} - T_{Sur}) - Q_{Dis}}{I(1 - 10^{-A})} \quad (2)$$

Here, η refers to the conversion efficiency at 1060 nm. T_{Max} is the maximum equilibrium temperature and T Sur is the ambient temperature. Q Dis is the energy generated by quartz cell and water upon laser irradiation, measured independently. I indicate laser power. A is the Absorbance of antler hat and antennas at 1060 nm. S is the surface area of cell and h is heat transfer coefficient. hS is calculated from substituting equations:

$$\theta = \frac{T - T_{Sur}}{T_{Max} - T_{Sur}} \quad (3)$$

θ is the driving force temperature during cooling period.

$$t = -\tau_s \ln \theta \quad (4)$$

τs is the time constant in cooling period

$$hS = \frac{mc}{\tau_s} \quad (5)$$

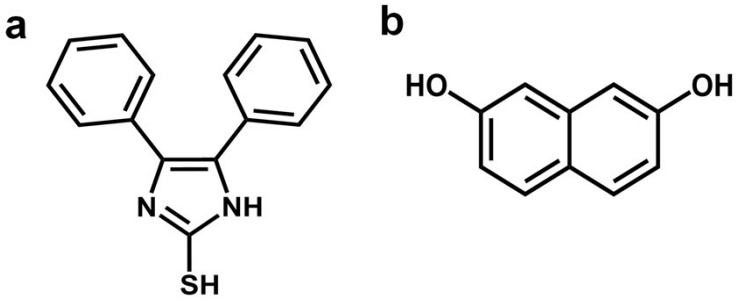

Figure S3. (a) The structural formula of DPI ligand. (b) The structural formula of DHN reductant.

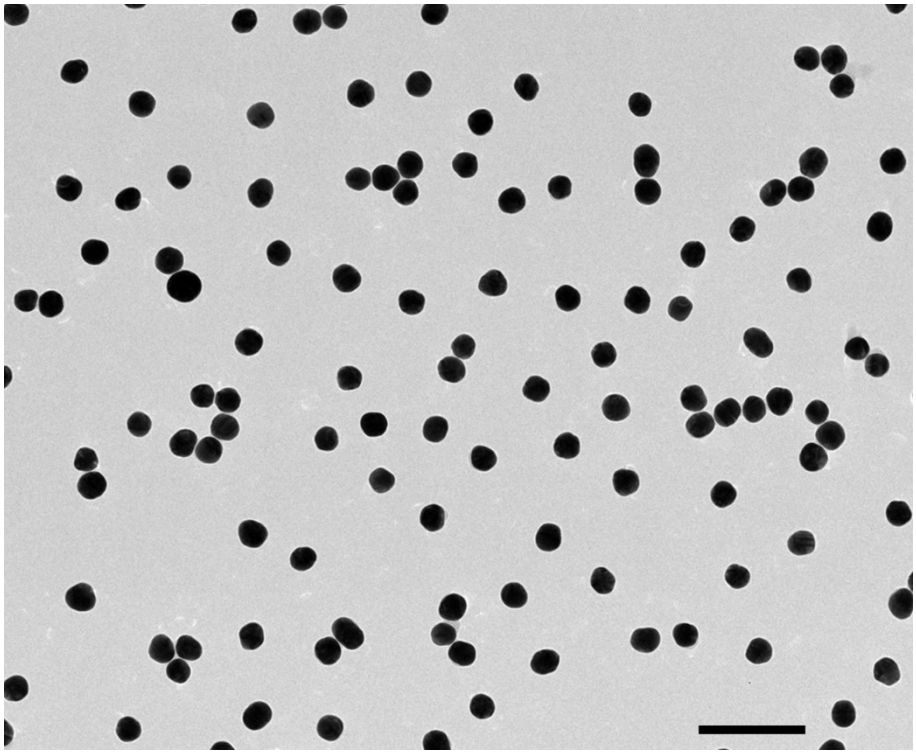

Figure S4. TEM image of citrate-stabilized 60 nm Au seed NPs. Scale bar: 250 nm

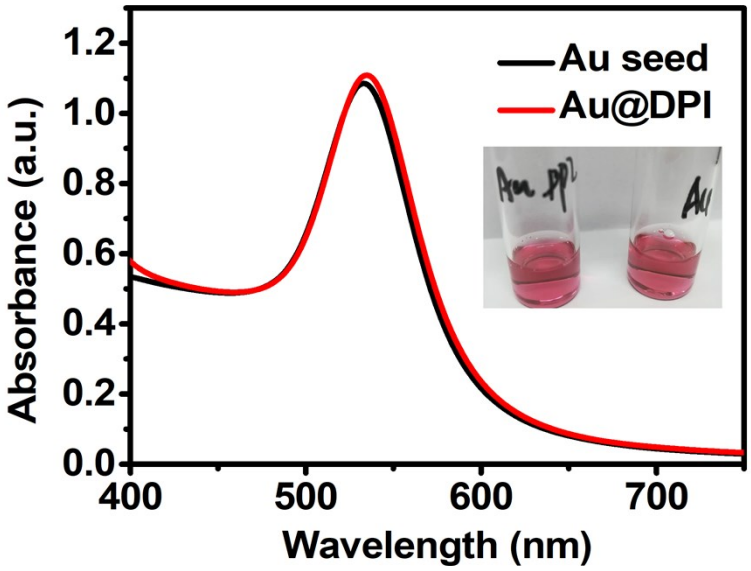

Figure S5. Absorption spectra of Au seeds before and after incubation with DPI ligand. Inset: photographs of the corresponding samples

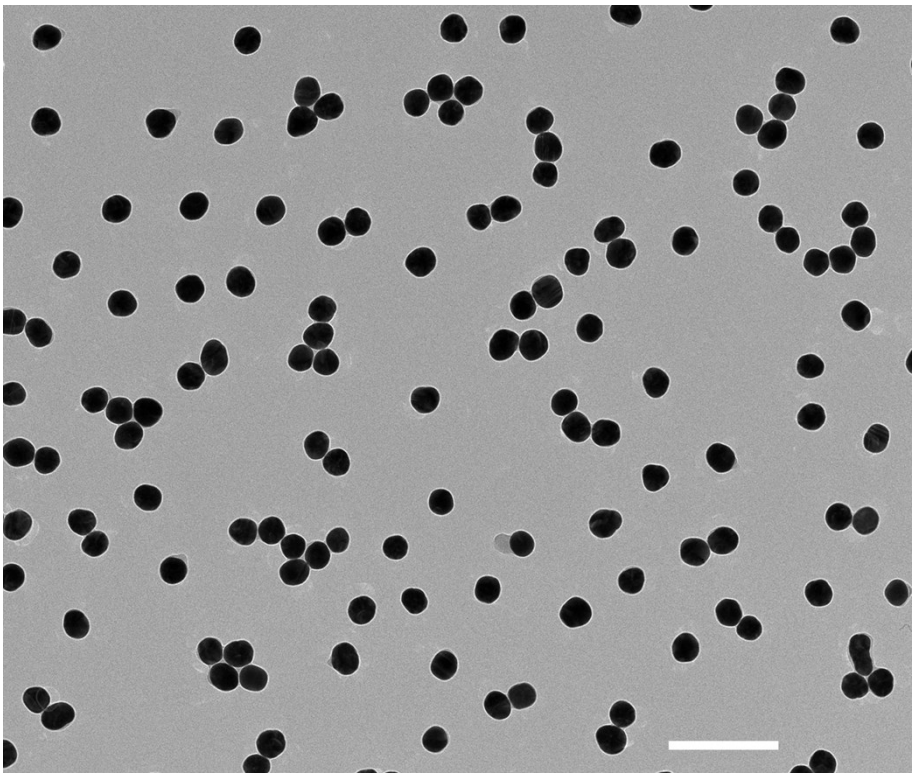

Figure S6. TEM image of MTAB-stabilized 60 nm Au seed NPs after incubating with DPI ligand. Scale bar: 250 nm.

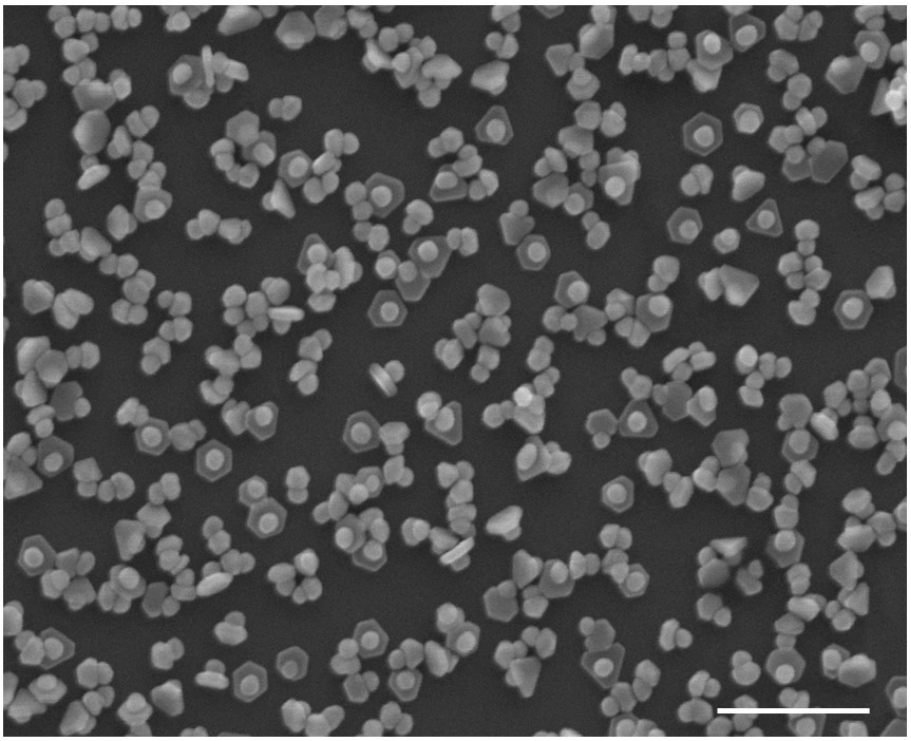

Figure S7. SEM image of mortarboard. Scale bar: 500 nm.

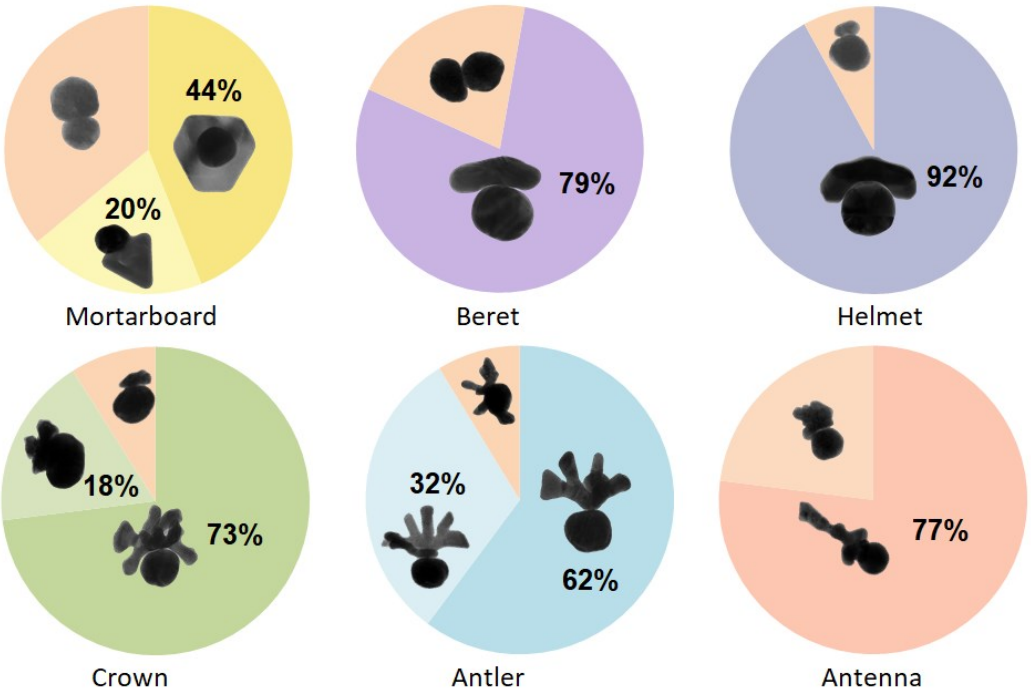

Figure S8. The statistics of the Au-on-Au Janus structures from the various growth modes.

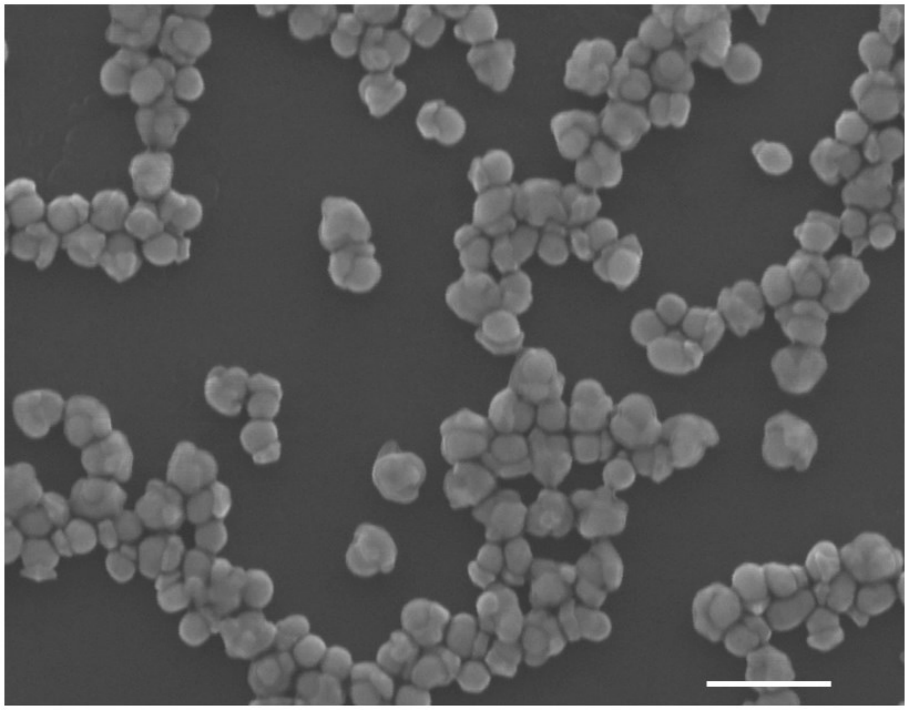

Figure S9. SEM image of helmet under [NaOH] = 3.96 mM. Scale bar: 250 nm

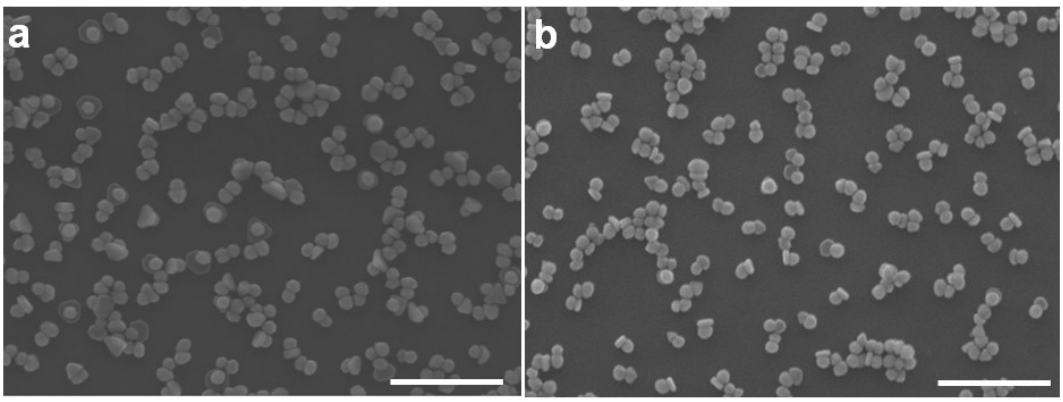

Figure S10. SEM image of hat nanostructure under different [NaOH]. (a) 1.26 mM (b) 1.98 mM. Scale bars: 500 nm.

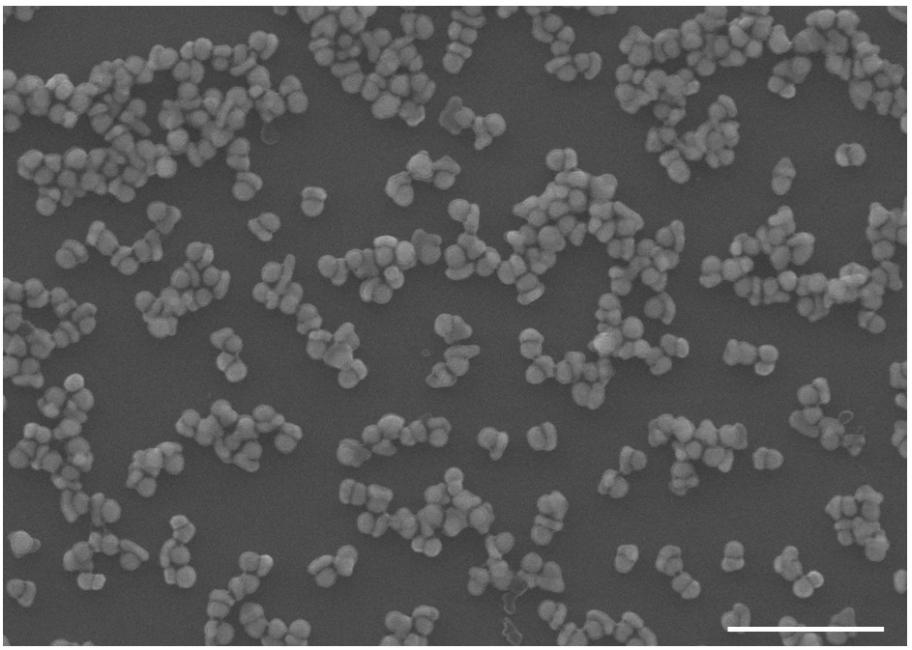

Figure S11. SEM image of beret hat structure. Scale bar: 500 nm

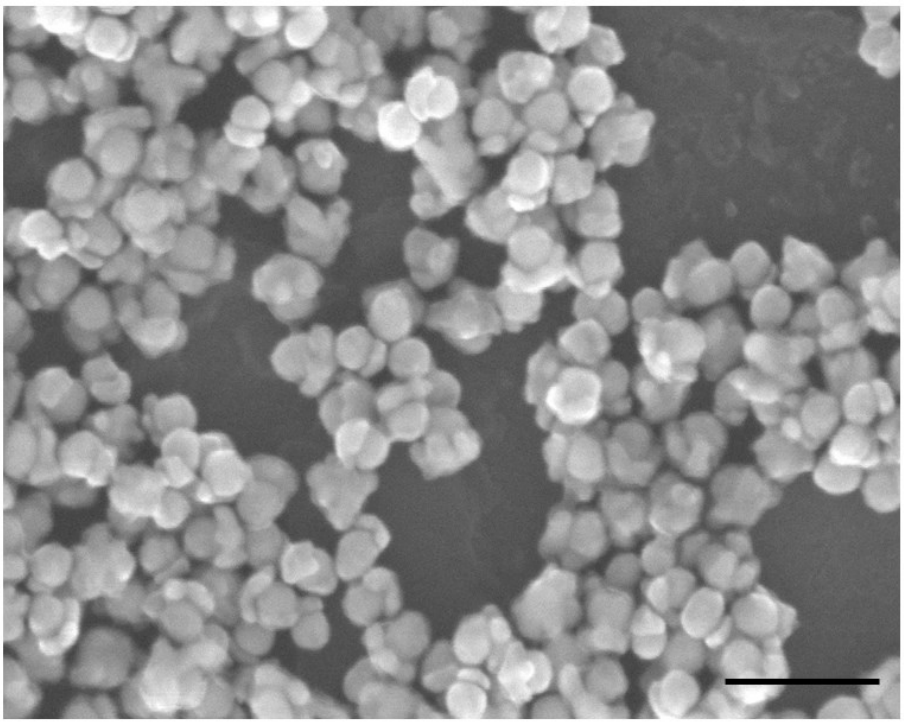

Figure S12. SEM image of helmet under [NaOH] = 6.6 mM. Scale bar: 250 nm

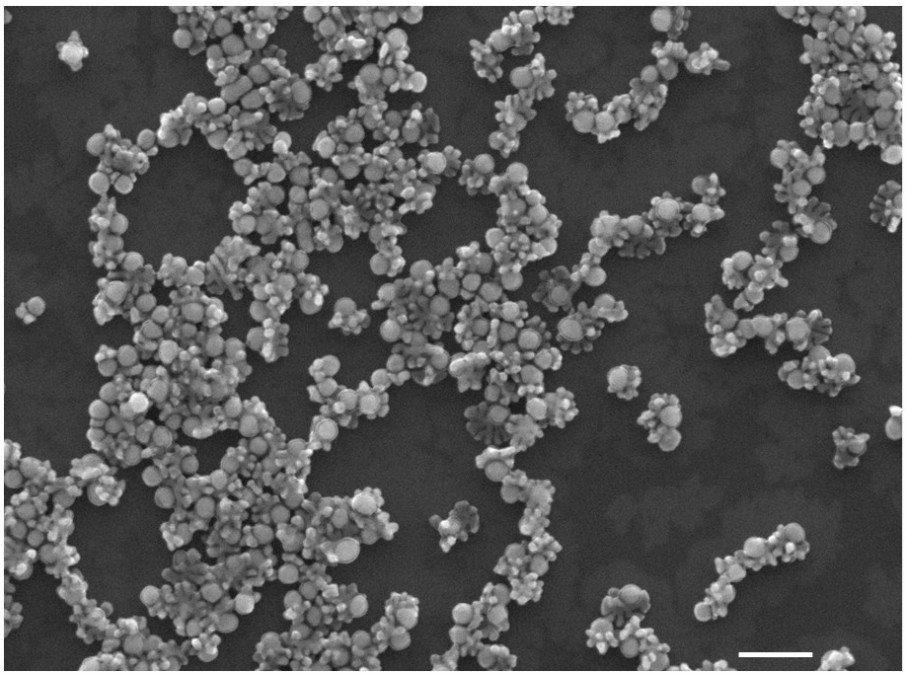

Figure S13. SEM image of crown structure. Scale bar: 250 nm.

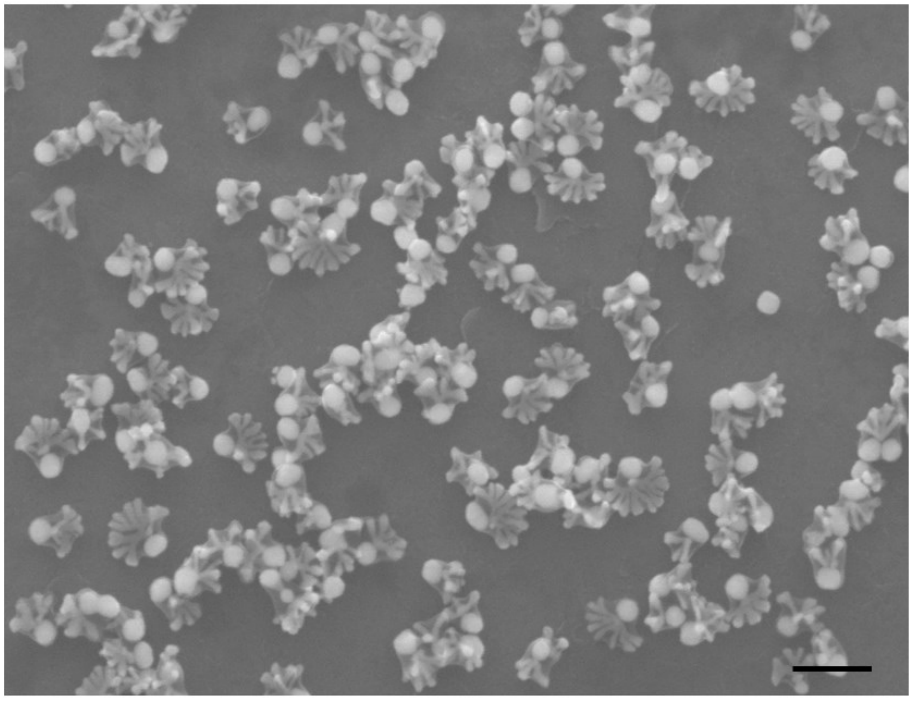

Figure S14. SEM image of antler hat structure. Scale bar: 250 nm.

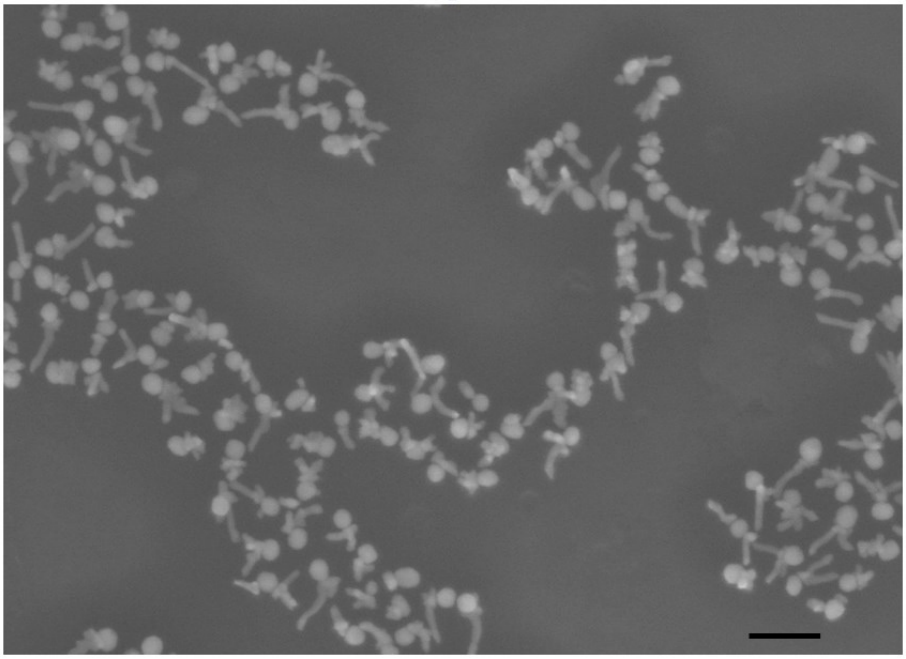

Figure S15. SEM image of antenna structure. Scale bar: 250 nm.

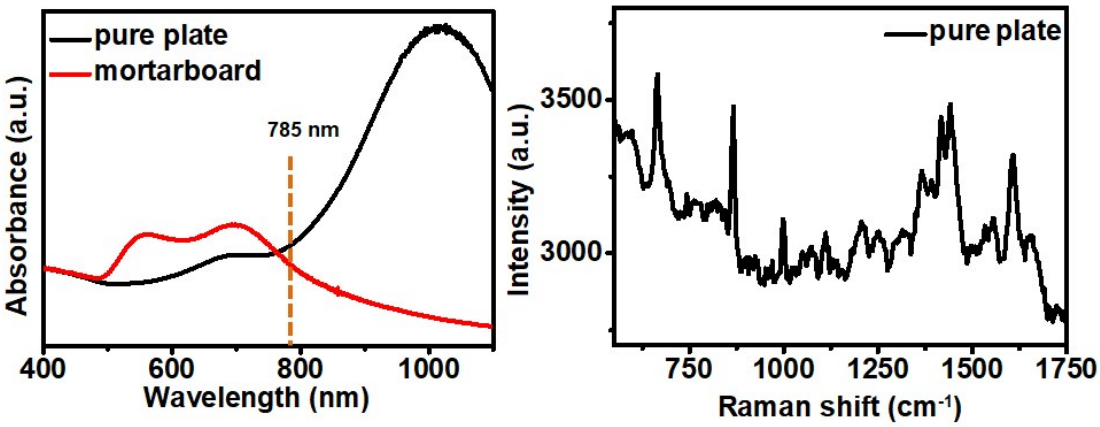

Figure S16. (a) Absorption spectra of mortarboard and pure Au nanoplates. (b) SERS spectra of pure Au nanoplate.

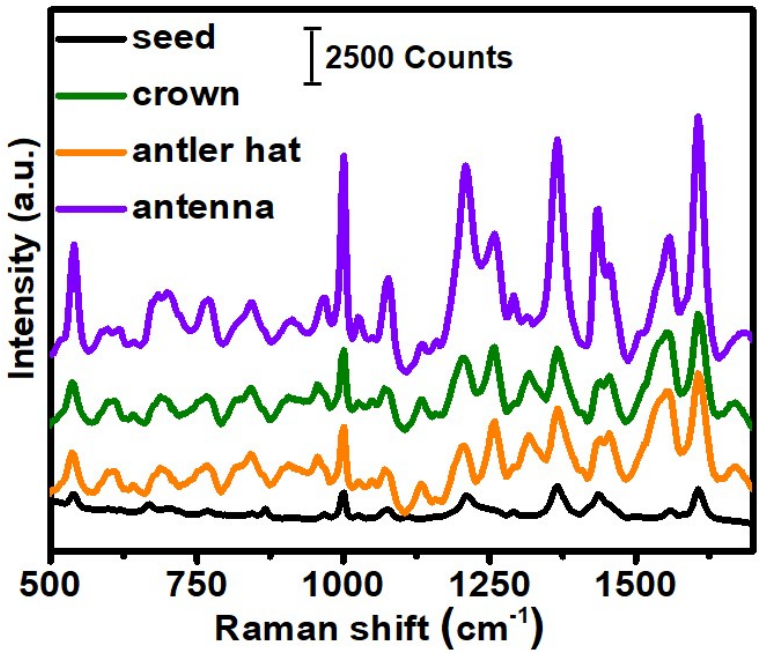

Figure S17. SERS spectra of the crown, antler hat, and antenna structures.

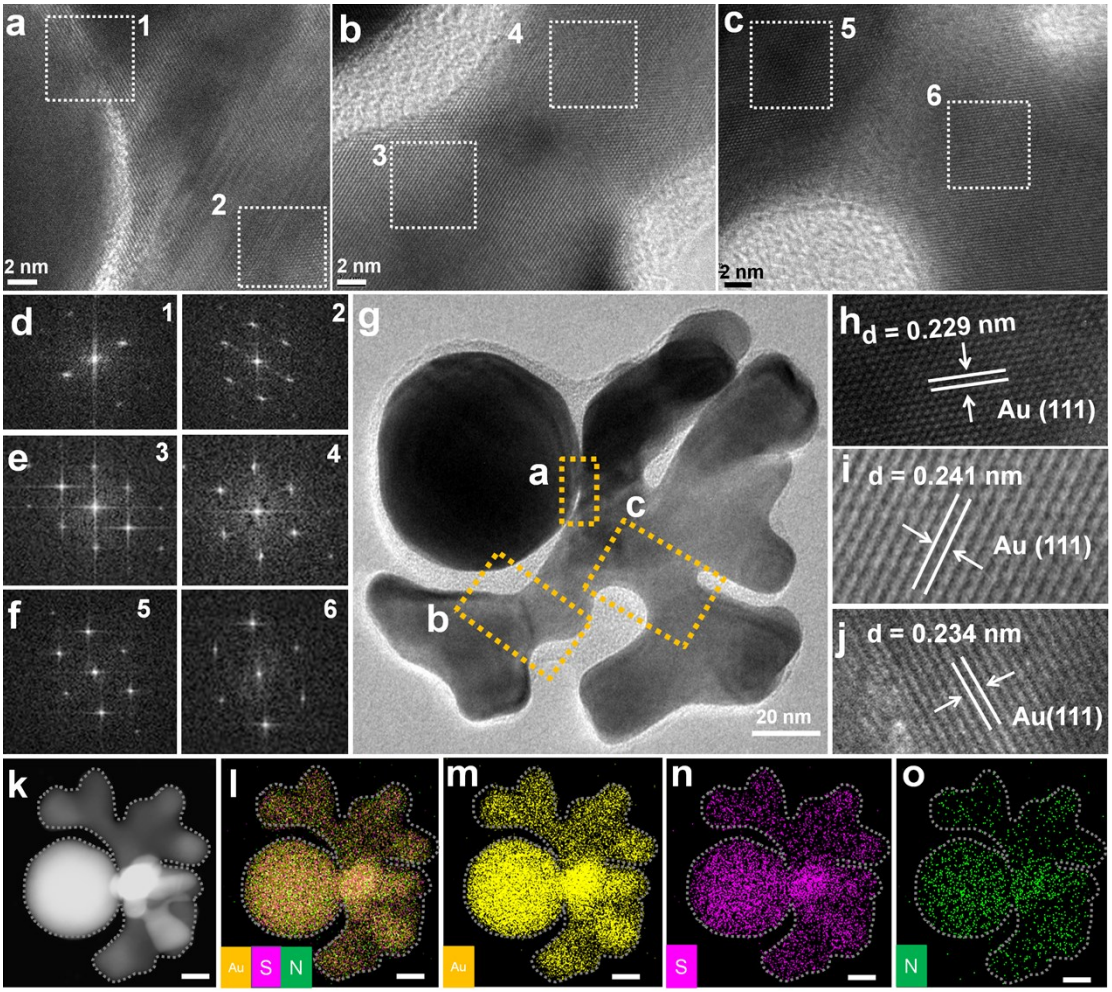

Figure S18. Enlarged Figure 4 in the main text.

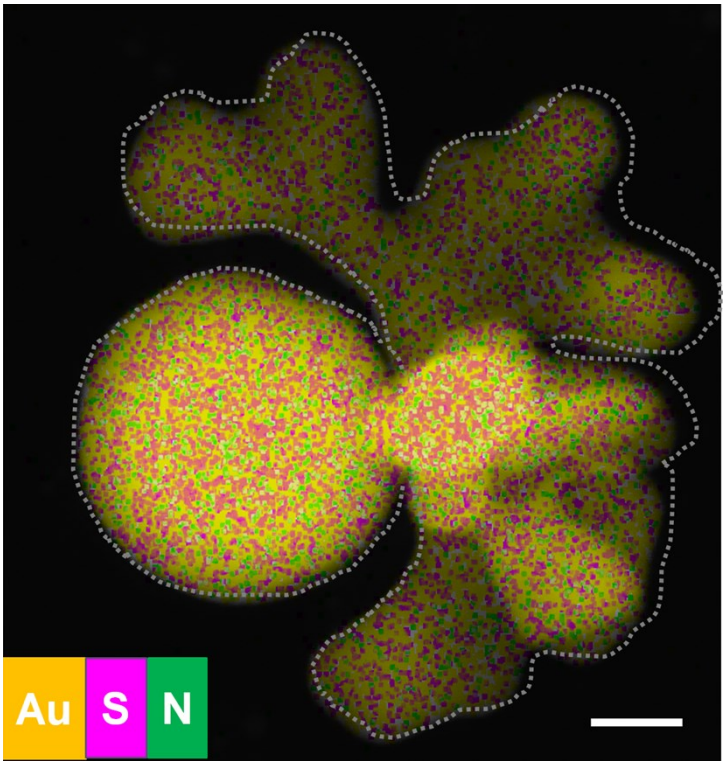

Figure S19. The overlay of the elemental mapping on the high-angle annular dark-field (HAADF) STEM image of the crown structure. The distribution of elements can be observed more clearly.

Nanostructures	Photothermal conversion efficiency (PTC%)/1064 nm	Reference
Au Nanomatryoshkas(Au/SiO_2/Au)	63%	ACS Nano 2014, 8, 6, 6372–6381
Au plasmonic blackbodies	80.8 %	ACS Nano 2018, 12, 2643−2651
Au Nanostar@MOF	48.5%	Nano Lett. 2019, 19, 6772−6780
Au wires-on-AuNR	67.2%	Angew. Chem. Int. Ed. 2020, 59, 14443–14448
Multi-branched Au nanocrystals	60%	J. Mater. Chem. B, 2020, 8, 5491-5499
Au-pDA@pDA	55.3%	Colloids and Surfaces A: Physicochemical and Engineering Aspects, 2021, 611, 125758
Au nanochains@SiO_2	82.2%	Adv. Mater., 2020, 2006532.
Au Antler hats	66.2%	This work

Table S2. Photothermal efficiencies of recently reported Au nanostructures.

Reference:

1 Y. Feng, Y. Wang, H. Wang, T. Chen, Y. Y. Tay, L. Yao, Q. Yan, S. Li and H. Chen, *Small*, 2012, **8**, 246-251.

2 G. Chen, Y. Wang, M. Yang, J. Xu, S. J. Goh, M. Pan and H. Chen, *J. Am. Chem. Soc*, 2010, **132**, 3644-3645.

3 (a) D. Chen, Z. Zhong, Q. Ma, J. Shao, W. Huang and X. Dong, *ACS Appl. Mater. & Inter*, 2020, **12**, 26914-26925. (b) P. Liang, H. Tang, R. Gu, L. Xue, D. Chen, W. Wang, Z. Yang, W. Si and X. Dong, *Sci. China. Mater*, 2019, **62**, 1199-1209. (c) D. Chen, Y. Tang, J. Zhu, J. Zhang, X. Song, W. Wang, J. Shao, W. Huang, P. Chen and X. Dong, *Biomaterials*, 2019, **221**, 119422. (d) Z. Yin, D. Chen, J. Zou, J. Shao, H. Tang, H. Xu, W. Si and X. Dong, *ChemistrySelect*, 2018, **3**, 4366-4373.